Supporting Information

Rational construction AIEgens with wide color tunability and their specific lipid droplets imaging applications

Fei Zhang,‡[a] Zhe Li,‡[b] Yaoming Liu,[c] Binsheng Yang,[a] Hui Qiao,[a] Jie Chai,[d] Guangming Wen[d] and Bin Liu*[a]

[a]*Institute of Molecular Science, Engineering Research Center for Sewage Treatment of Shanxi Province, Shanxi University, Taiyuan, China, 030006. E-mail: liubin@sxu.edu.cn.* [b]*The Second People's Hospital of Shanxi Province, Taiyuan, China.* [c]*Scientific Instrument Center of Shanxi University, Taiyuan, China.* [d]*Department of Chemistry, Jinzhong University, Taiyuan, 030619, China.*

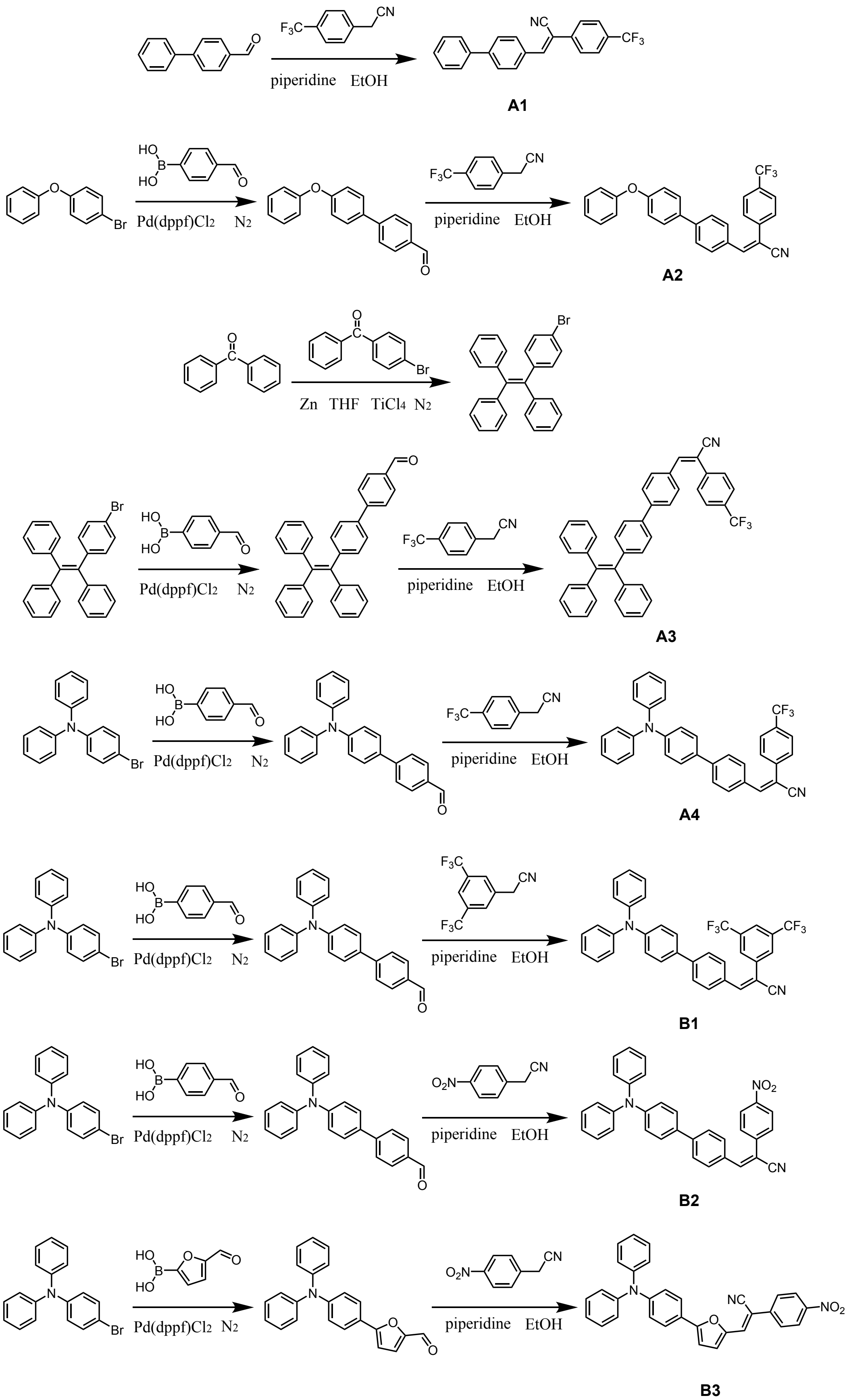

Scheme S1 Synthetic routes to AIEgens with widely tunable emissions.

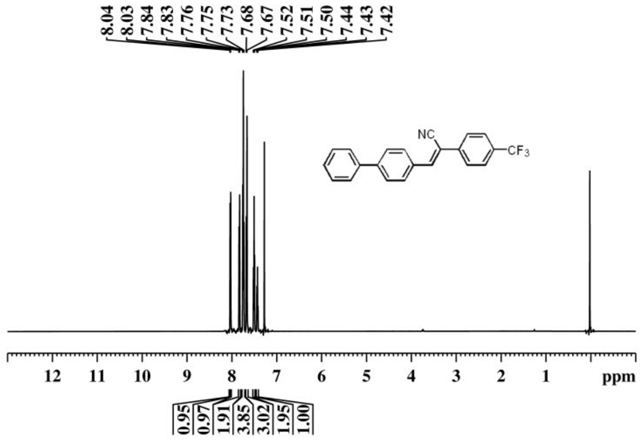

Fig. S1. ^{1}H NMR spectrum of **A1**.

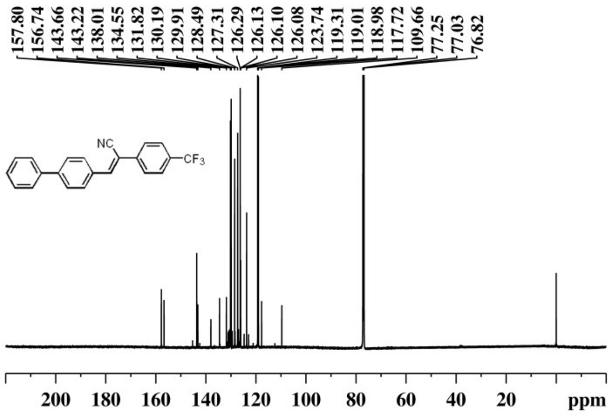

Fig. S2 ^{13}C NMR spectrum of **A1**.

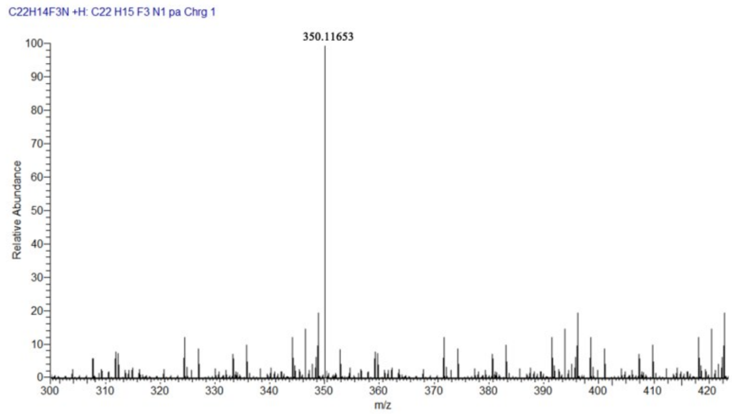

Fig. S3 ESI-MS spectrum of **A1**.

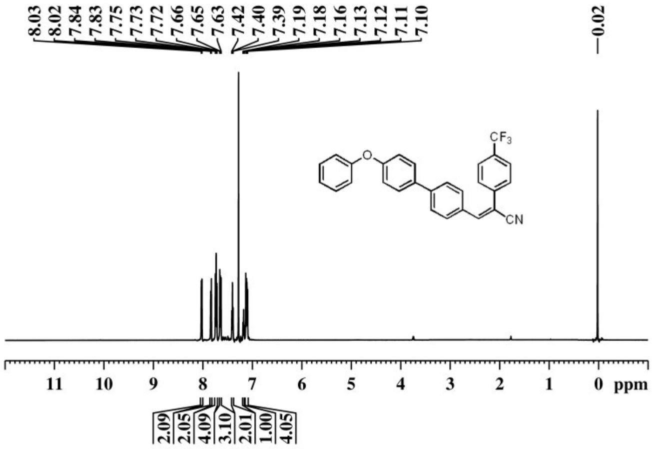

Fig. S4 ^{1}H NMR spectrum of **A2**.

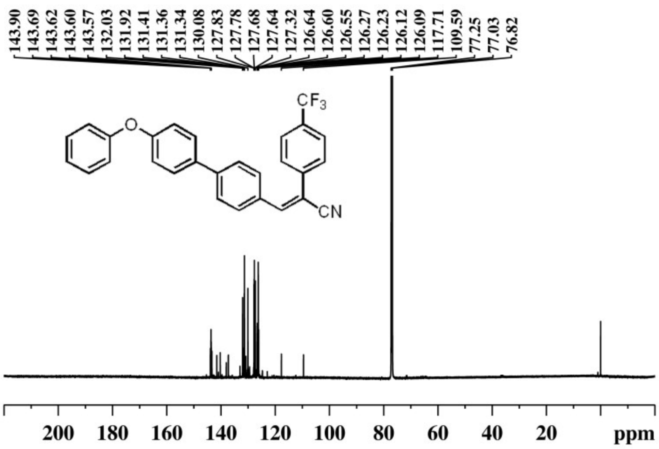

Fig. S5 ^{13}C NMR spectrum of **A2**.

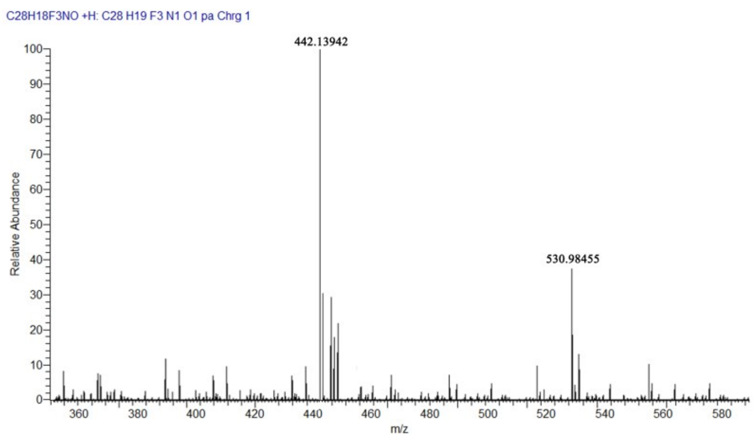

Fig. S6 ESI-MS spectrum of **A2**.

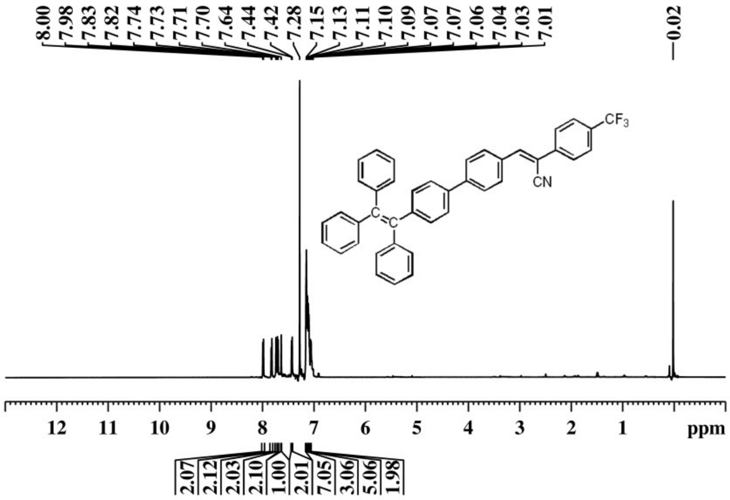

Fig. 7 ^{1}H NMR spectrum of **A3**.

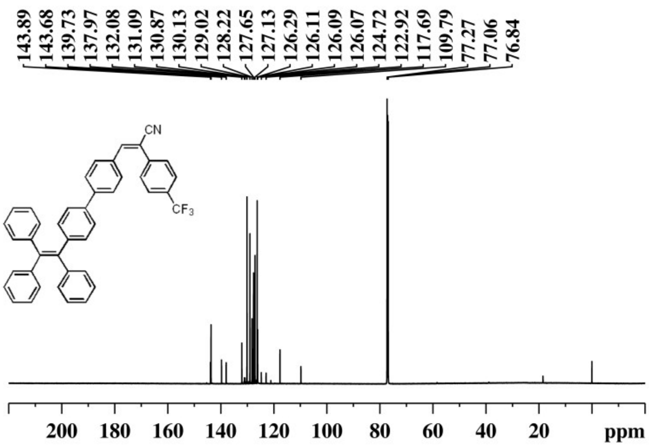

Fig. S8 ^{13}C NMR spectrum of **A3**.

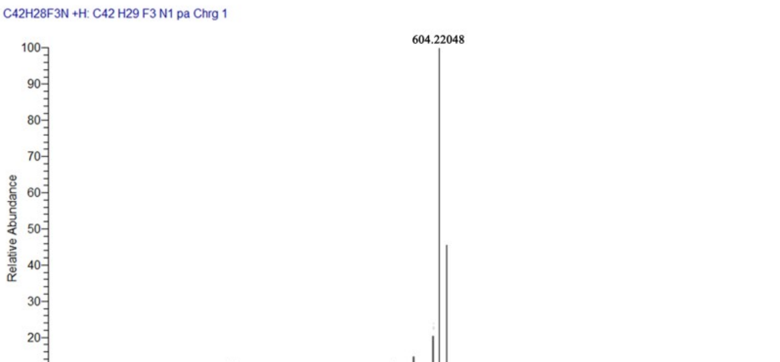

Fig. S9 ESI-MS spectrum of **A3**.

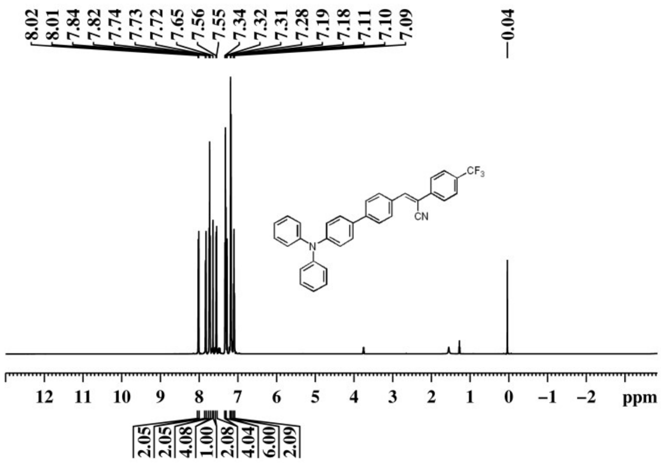

Fig. 10 ^{1}H NMR spectrum of **A4**.

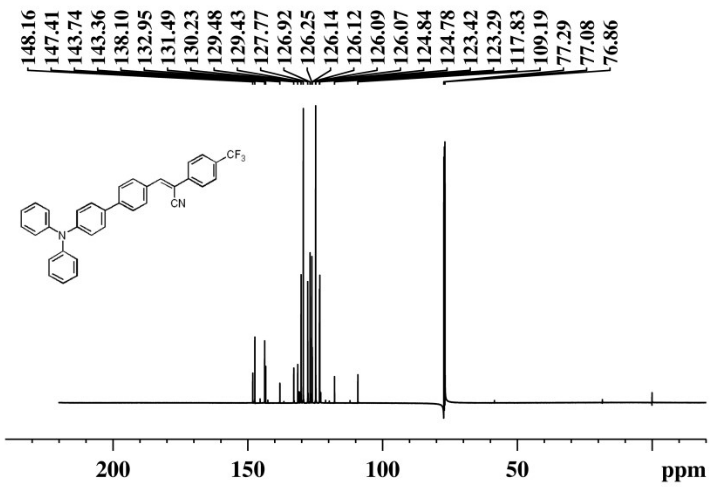

Fig. S11 ^{13}C NMR spectrum of **A4**.

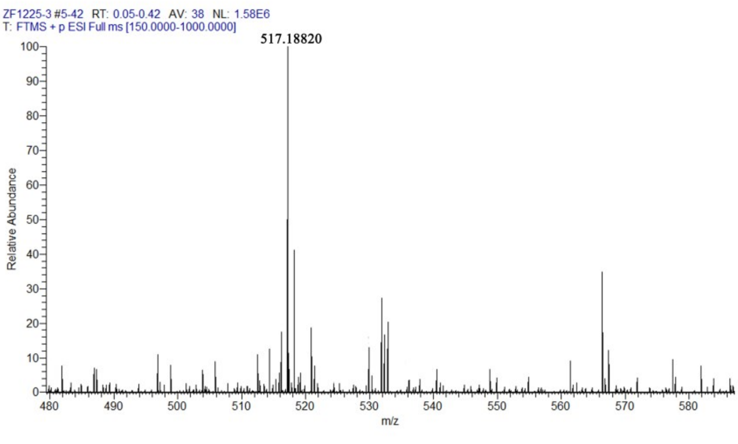

Fig. S12 ESI-MS spectrum of **A4**.

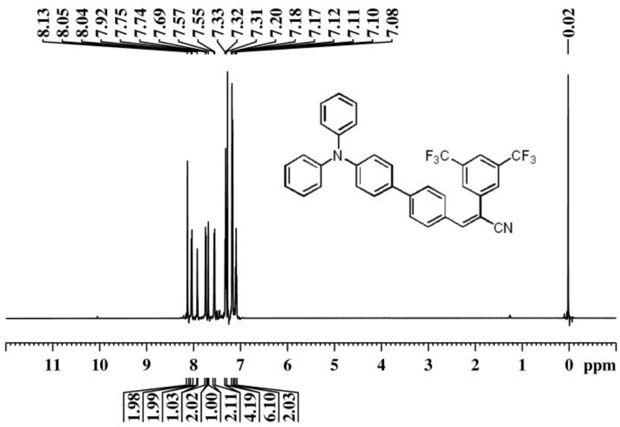

Fig. 13 ^{1}H NMR spectrum of **B1**.

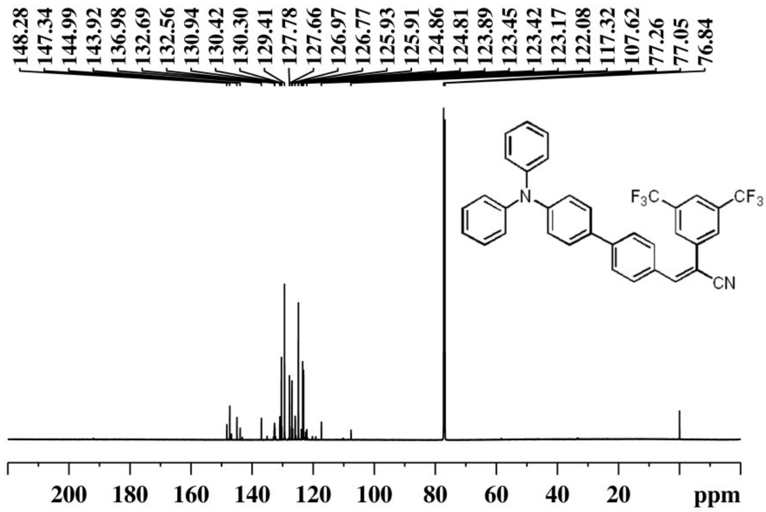

Fig. S14 ^{13}C NMR spectrum of **B1**.

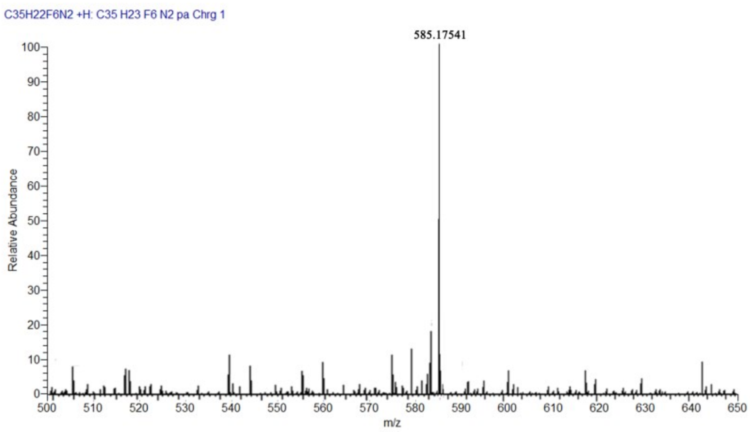

Fig. S15 ESI-MS spectrum of **B1**.

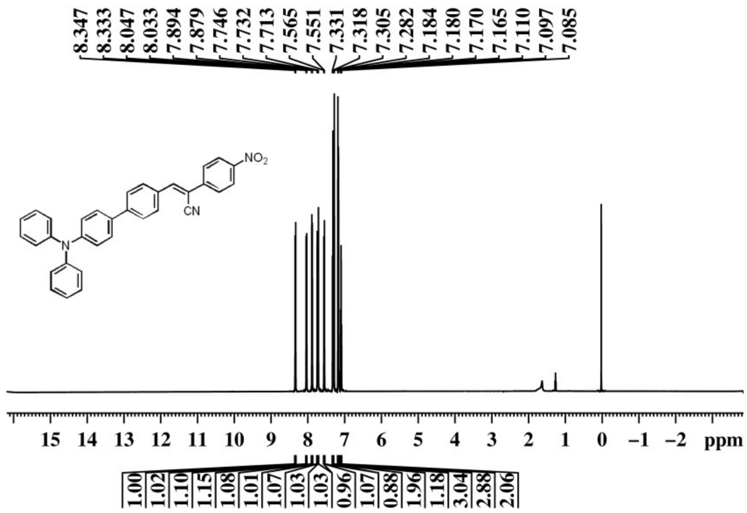

Fig. 16 [1]H NMR spectrum of **B2**.

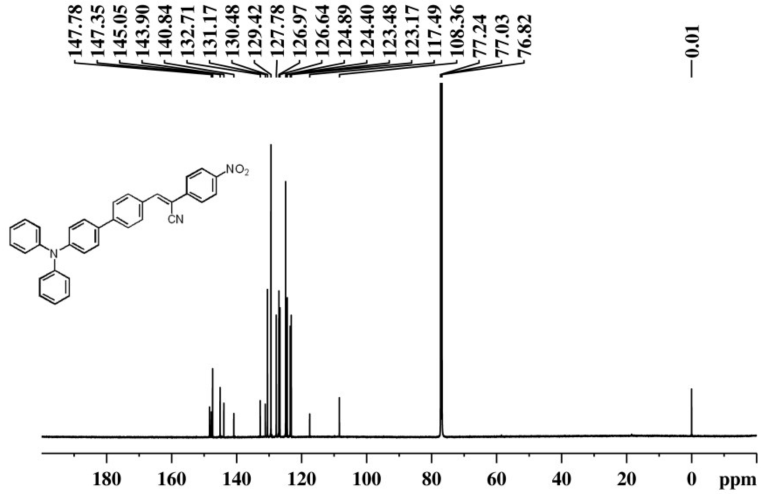

Fig. S17 [13]C NMR spectrum of **B2**.

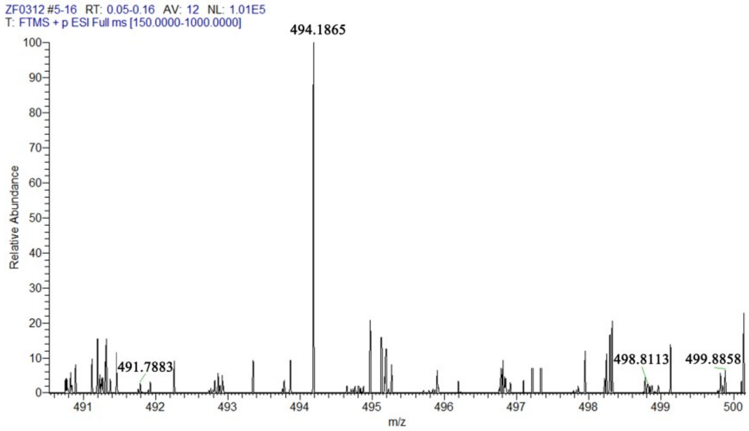

Fig. S18 ESI-MS spectrum of **B2**.

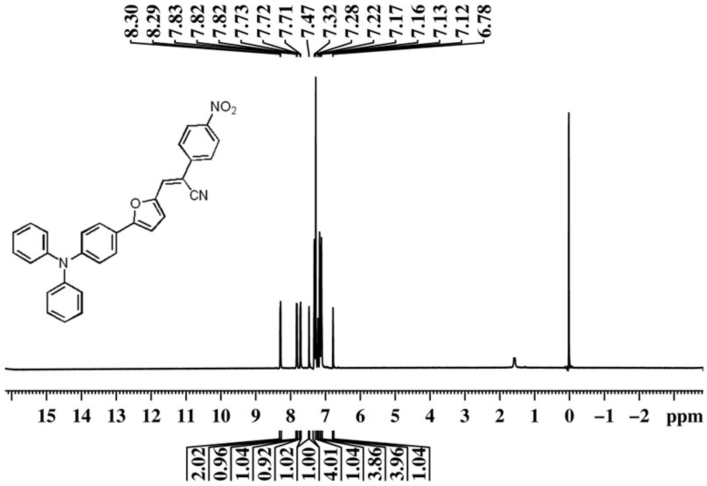

Fig. 19 ^{1}H NMR spectrum of **B3**.

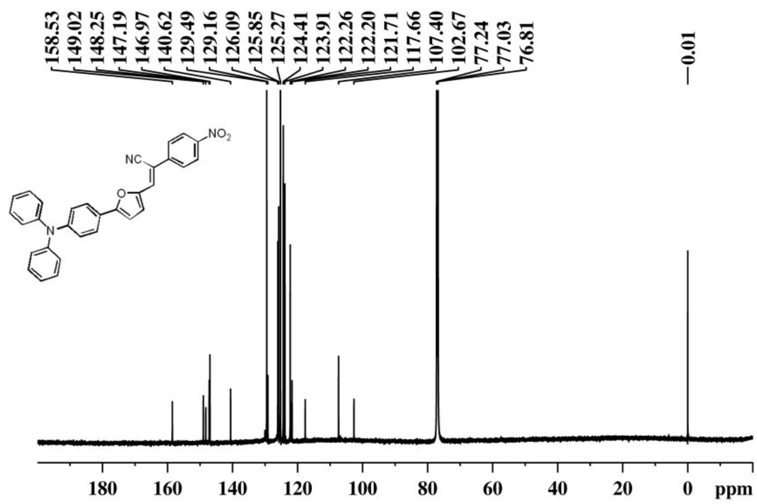

Fig. S20 ^{13}C NMR spectrum of **B3**.

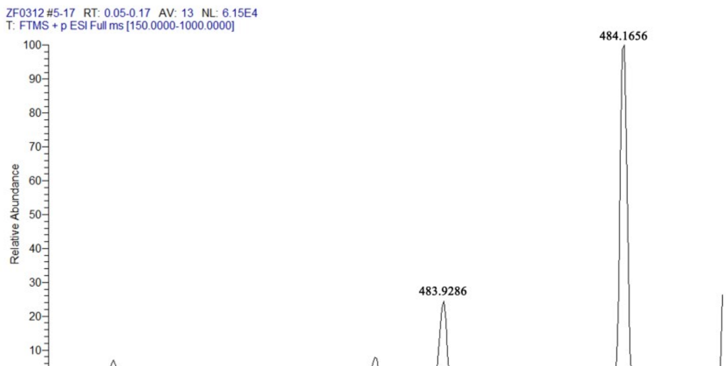

Fig. S21 ESI-MS spectrum of **B3**.

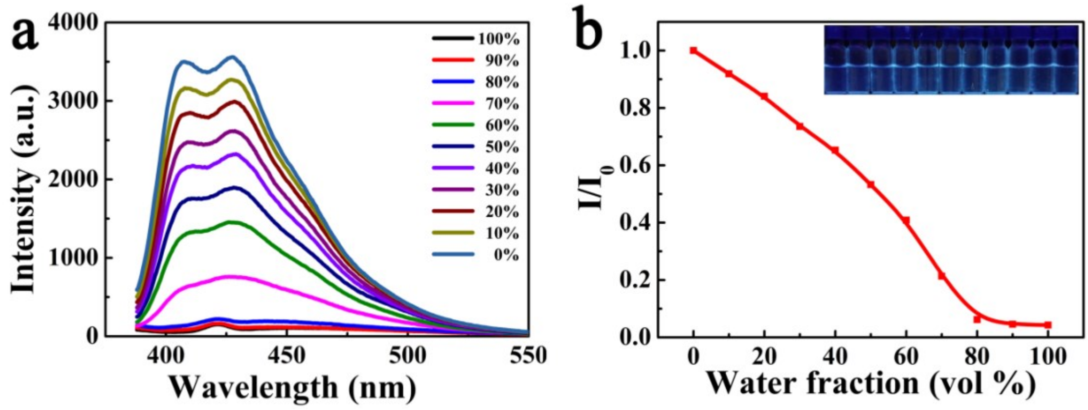

Fig. S22 (a) PL spectra of **A1** in DMSO solution with different water fractions (f_w). (b) Plots of the relative emission intensity (I/I_0) versus f_w in DMSO/water mixture of **A1**. Insert: fluorescent photographs of **A1** in DMSO solution with different water fractions.

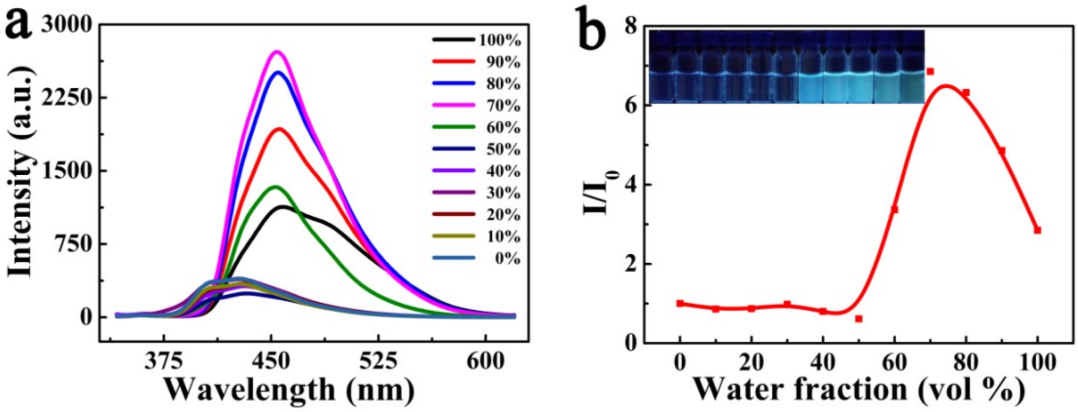

Fig. S23 (a) PL spectra of **A2** in DMSO solution with different water fractions (f_w). (b) Plots of the relative emission intensity (I/I_0) versus f_w in DMSO/water mixture of **A2**. Insert: fluorescent photographs of **A2** in DMSO solution with different water fractions.

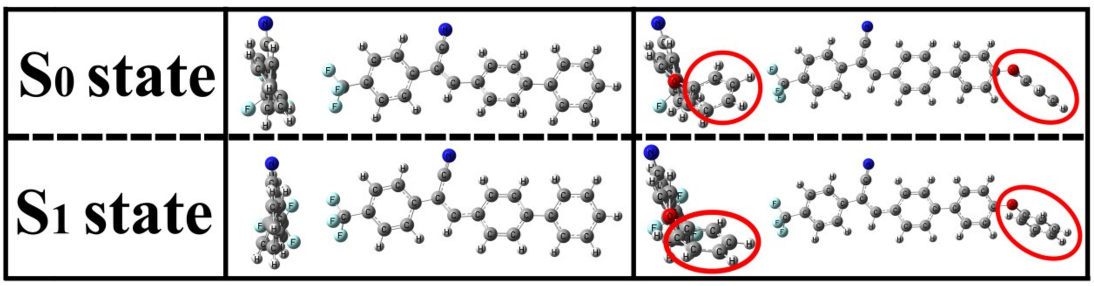

Fig. S24 Optimized structures of **A1** (left) and **A2** (right) in the S_0 and S_1 states.

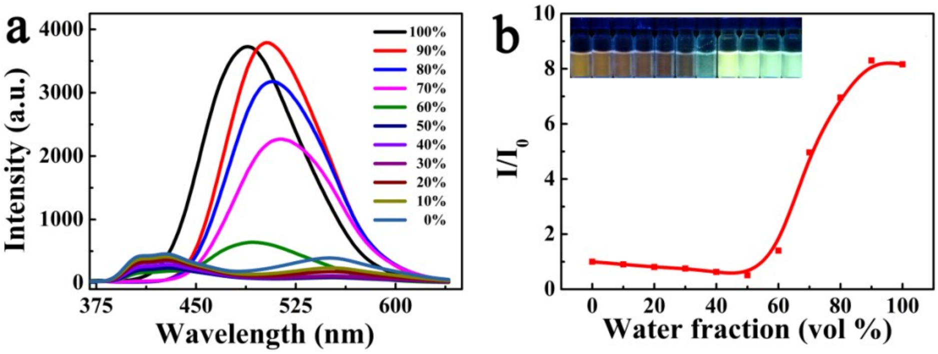

Fig. S25 (a) PL spectra of **A3** in DMSO solution with different water fractions (f_w). (b) Plots of the relative emission intensity (I/I_0) versus f_w in DMSO/water mixture of **A3**. Insert: fluorescent photographs of **A3** in DMSO solution with different water fractions.

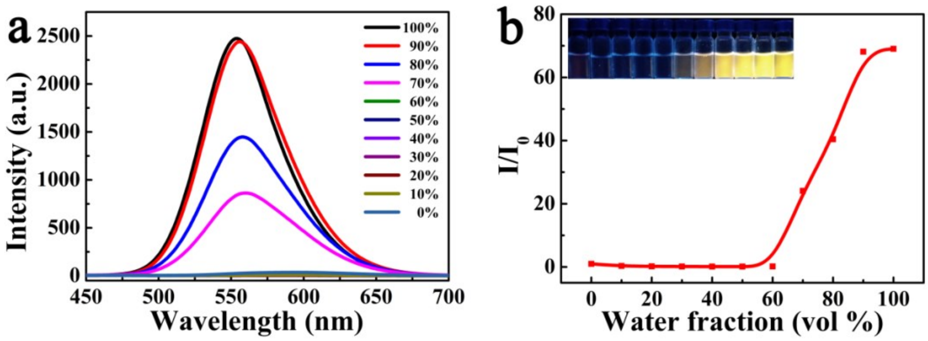

Fig. S26 (a) PL spectra of **A4** in DMSO solution with different water fractions (f_w). (b) Plots of the relative emission intensity (I/I_0) versus f_w in DMSO/water mixture of **A4**. Insert: fluorescent photographs of **A4** in DMSO solution with different water fractions.

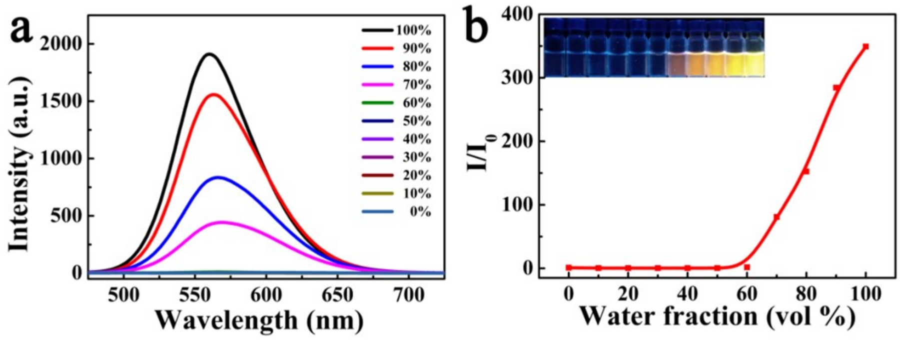

Fig. S27 (a) PL spectra of **B1** in DMSO solution with different water fractions (f_w). (b) Plots of the relative emission intensity (I/I_0) versus f_w in DMSO/water mixture of **B1**. Insert: fluorescent photographs of **B1** in DMSO solution with different water fractions.

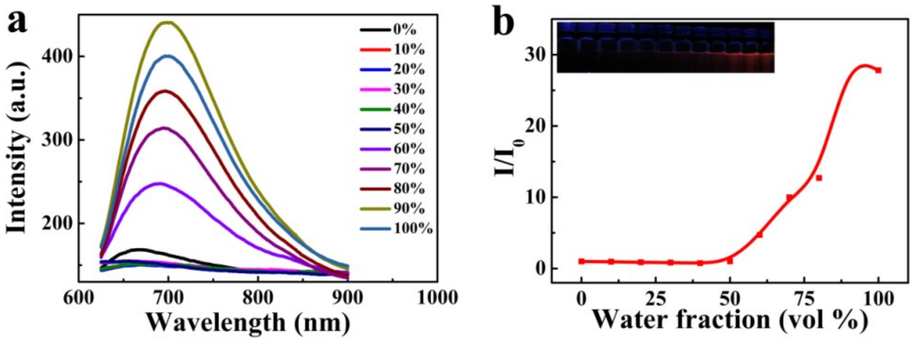

Fig. S28 (a) PL spectra of **B2** in DMSO solution with different water fractions (f_w). (b) Plots of the relative emission intensity (I/I_0) versus f_w in DMSO/water mixture of **B2**. Insert: fluorescent photographs of **B2** in DMSO solution with different water fractions.

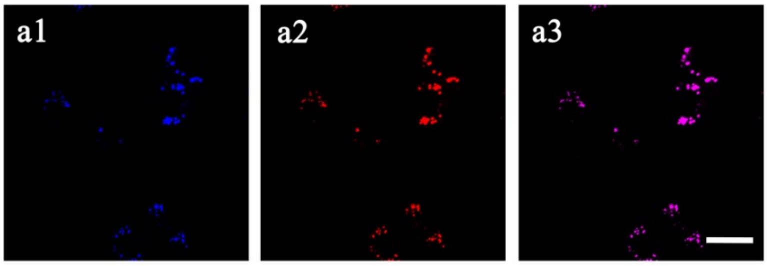

Fig. S29 Co-localization imaging of PC 12 cells stained with **A2** and Nile Red. (a) Blue channel, (b) Red channel, (c) Merged images of panels (a) and (b). For **A2**, λ_{ex} = 405 nm, λ_{em} = 420–480 nm; For Nile Red, λ_{ex} = 514 nm, λ_{em} = 580–650 nm. Concentration: **A2** (1.0×10^{-6} M), Nile Red (1.0×10^{-6} M). Scale bar: 5 μm. Pearson's correlation coefficient: 0.94.

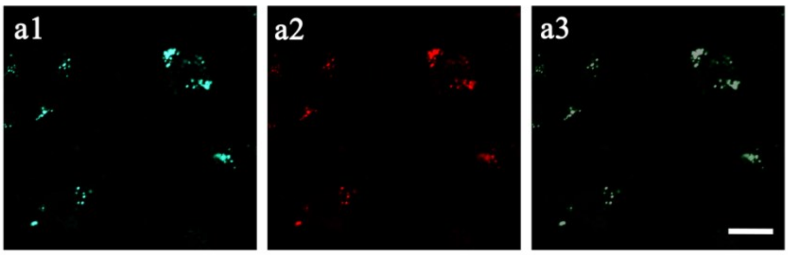

Fig. S30 Co-localization imaging of PC 12 cells stained with **A3** and Nile Red. (a) Green channel, (b) Red channel, (c) Merged images of panels (a) and (b). For **A3**, λ_{ex} = 458 nm, λ_{em} = 460–540 nm; For Nile Red, λ_{ex} = 514 nm, λ_{em} = 580–650 nm. Concentration: **A3** (1.0×10^{-6} M), Nile Red (1.0×10^{-6} M). Scale bar: 5 μm. Pearson's correlation coefficient: 0.92.

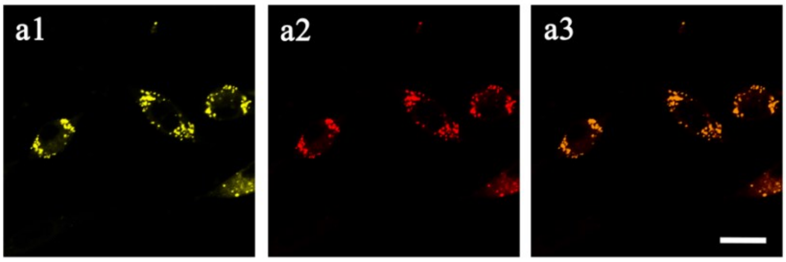

Fig. S31 Co-localization imaging of PC 12 cells stained with **A4** and Nile Red. (a) Yellow channel, (b) Red channel, (c) Merged images of panels (a) and (b). For **A4**, λ_{ex} = 514 nm, λ_{em} = 520–570 nm; For Nile Red, λ_{ex} = 514 nm, λ_{em} = 590–650 nm. Concentration: **A4** (1.0×10^{-6} M), Nile Red (1.0×10^{-6} M). Scale bar: 5 μm. Pearson's correlation coefficient: 0.88.

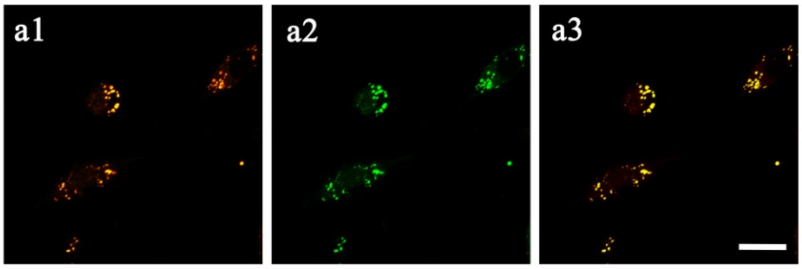

Fig. S32 Co-localization imaging of PC 12 cells stained with **B1** and BODIPY 493/503 Green. (a) Orange channel, (b) Green channel, (c) Merged images of panels (a) and (b). For **B1**, λ_{ex} = 514 nm, λ_{em} = 540–620 nm; For BODIPY 493/503 Green, λ_{ex} = 488 nm, λ_{em} = 500–530 nm. Concentration: **B1** (1.0×10^{-6} M), BODIPY 493/503 Green (1.0×10^{-6} M). Scale bar: 5 μm. Pearson's correlation coefficient: 0.86.

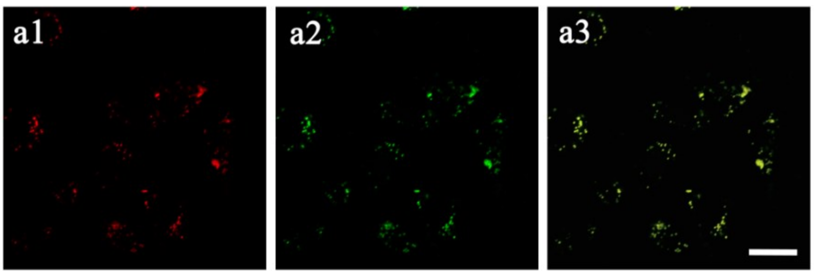

Fig. S33 Co-localization imaging of PC 12 cells stained with **B2** and BODIPY 493/503 Green. (a) Red channel, (b) Green channel, (c) Merged images of panels (a) and (b). For **B2**, λ_{ex} = 514 nm, λ_{em} = 590–680 nm; For BODIPY 493/503 Green, λ_{ex} = 488 nm, λ_{em} = 500–550 nm. Concentration: **B2** (1.0×10^{-6} M), BODIPY 493/503 Green (1.0×10^{-6} M). Scale bar: 5 μm. Pearson's correlation coefficient: 0.91.

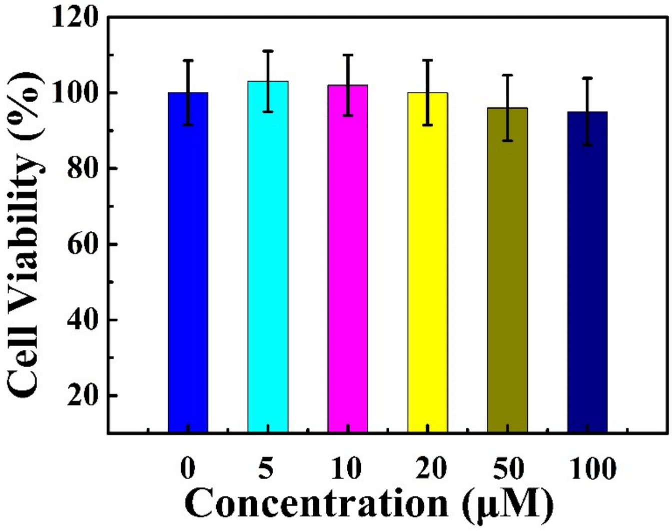

Fig. S34 The cytotoxicity on Hela cells in different concentration of **A2**.

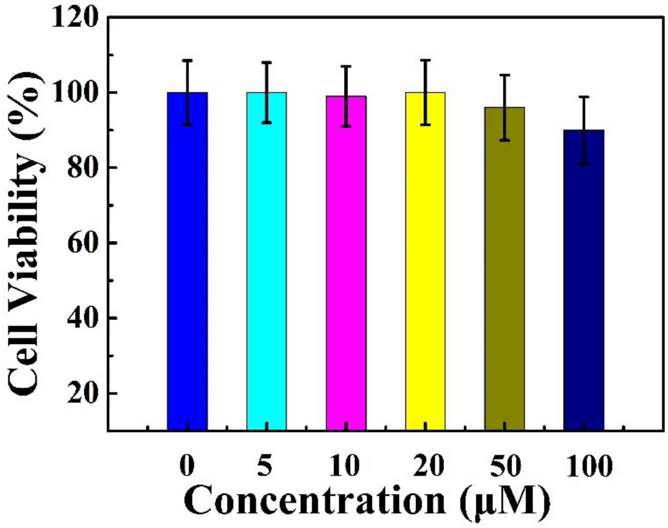

Fig. S35 The cytotoxicity on Hela cells in different concentration of **A3**.

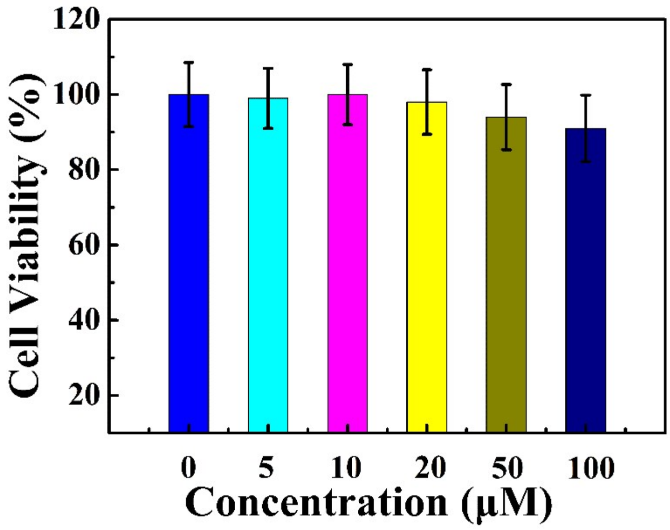

Fig. S36 The cytotoxicity on Hela cells in different concentration of **A4**.

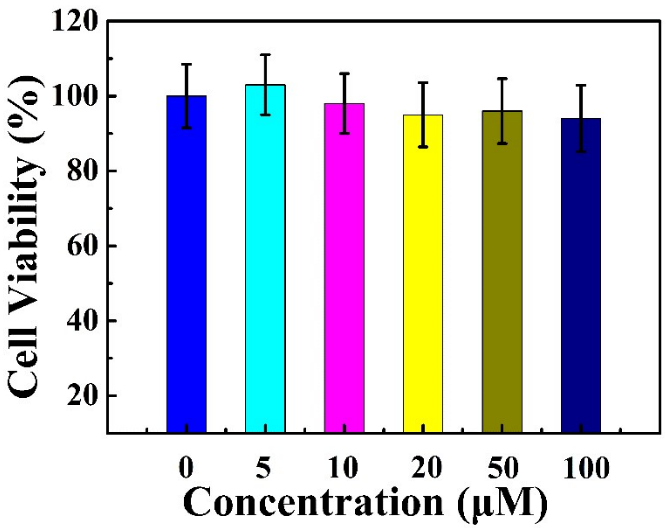

Fig. S37 The cytotoxicity on Hela cells in different concentration of **B1**.

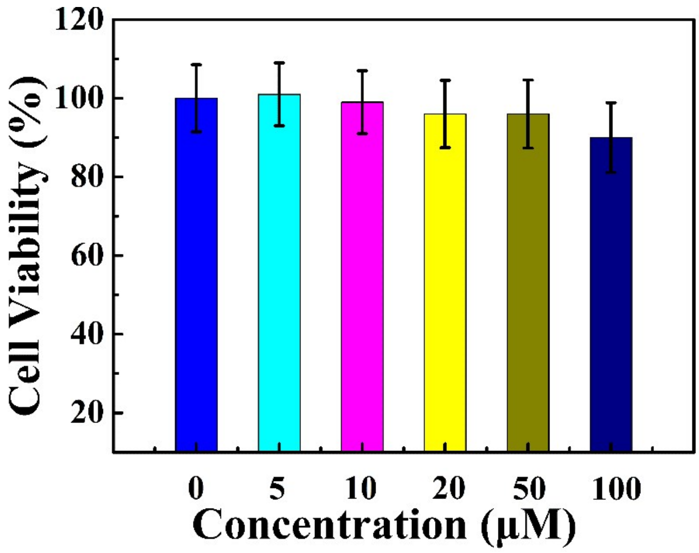

Fig. S38 The cytotoxicity on Hela cells in different concentration of **B2**.

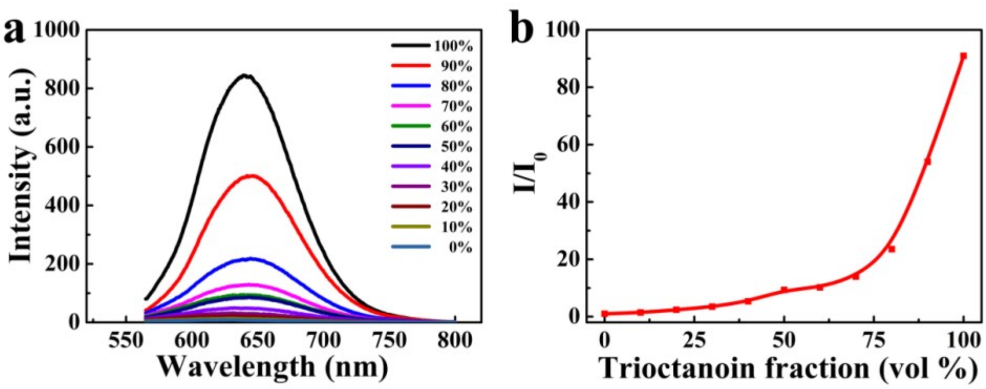

Fig. S39 (a) Emission spectra of **B3** in the mixed solvent of methanol and trioctanoin at different trioctanoin fractions (f_T). (b) Plot of relative emission intensity (I/I_0) versus f_T of **B3**.

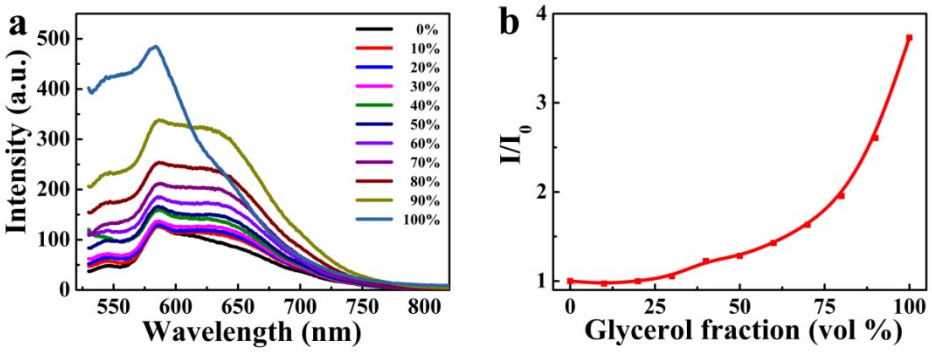

Fig. S40 (a) Emission spectra of **B3** in the mixed solvent of methanol and glycerol at different glycerol fractions (f_G). (b) Plot of relative emission intensity (I/I_0) versus f_G of **B3**.

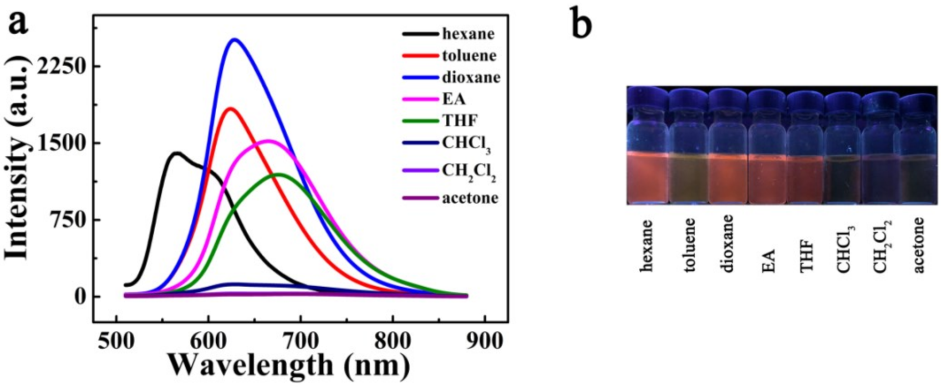

Fig. S41 (a) PL spectra of **B3** in various solvents. Concentration: 1 μM; excitation wavelength: 495 nm. (b) Photographs: showing the solution under 365 nm UV light.

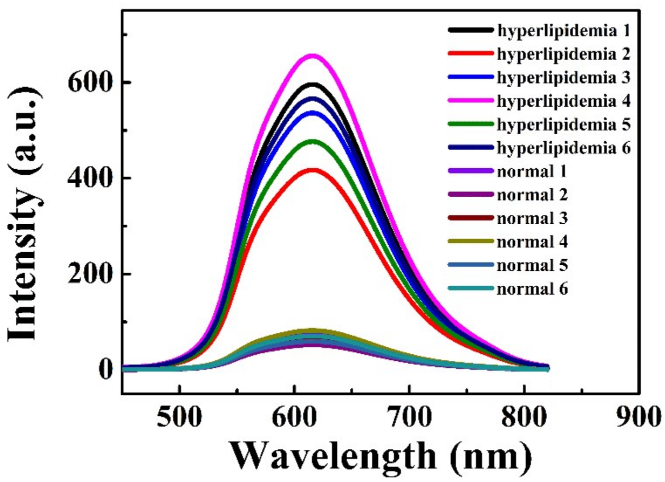

Fig. S42 Emission spectra of **B3** in the serum of hyperlipidemia (1−6) and normal people (1−6).